

Evolving Hard Maximum Cut Instances for Quantum Approximate Optimization Algorithms

Shuaiqun Pan
LIACS, Leiden University
Leiden, The Netherlands
s.pan@liacs.leidenuniv.nl

Yash J. Patel
LIACS, Leiden University
Leiden, The Netherlands
y.j.patel@liacs.leidenuniv.nl

Aneta Neumann
The University of Adelaide
Adelaide, Australia
aneta.neumann@adelaide.edu.au

Frank Neumann
The University of Adelaide
Adelaide, Australia
frank.neumann@adelaide.edu.au

Thomas Bäck
LIACS, Leiden University
Leiden, The Netherlands
t.h.w.baeck@liacs.leidenuniv.nl

Hao Wang
LIACS, Leiden University
Leiden, The Netherlands
h.wang@liacs.leidenuniv.nl

ABSTRACT

Variational quantum algorithms, such as the Recursive Quantum Approximate Optimization Algorithm (RQAOA), have become increasingly popular, offering promising avenues for employing Noisy Intermediate-Scale Quantum devices to address challenging combinatorial optimization tasks like the maximum cut problem. In this study, we utilize an evolutionary algorithm equipped with a unique fitness function. This approach targets hard maximum cut instances within the latent space of a Graph Autoencoder, identifying those that pose significant challenges or are particularly tractable for RQAOA, in contrast to the classic Goemans and Williamson algorithm. Our findings not only delineate the distinct capabilities and limitations of each algorithm but also expand our understanding of RQAOA's operational limits. Furthermore, the diverse set of graphs we have generated serves as a crucial benchmarking asset, emphasizing the need for more advanced algorithms to tackle combinatorial optimization challenges. Additionally, our results pave the way for new avenues in graph generation research, offering exciting opportunities for future explorations.

KEYWORDS

variational quantum algorithms, RQAOA, Goemans and Williamson algorithm, graph autoencoder

ACM Reference Format:

Shuaiqun Pan, Yash J. Patel, Aneta Neumann, Frank Neumann, Thomas Bäck, and Hao Wang. 2025. Evolving Hard Maximum Cut Instances for Quantum Approximate Optimization Algorithms. In *Genetic and Evolutionary Computation Conference (GECCO '25)*, July 14–18, 2025, Malaga, Spain. ACM, New York, NY, USA, 11 pages. <https://doi.org/XXXXXXX.XXXXXXX>

Permission to make digital or hard copies of all or part of this work for personal or classroom use is granted without fee provided that copies are not made or distributed for profit or commercial advantage and that copies bear this notice and the full citation on the first page. Copyrights for components of this work owned by others than ACM must be honored. Abstracting with credit is permitted. To copy otherwise, or republish, to post on servers or to redistribute to lists, requires prior specific permission and/or a fee. Request permissions from permissions@acm.org.
GECCO '25, July 14–18, 2025, Malaga, Spain

© 2025 Association for Computing Machinery.
ACM ISBN 978-1-4503-XXXX-X/18/06...\$15.00
<https://doi.org/XXXXXXX.XXXXXXX>

1 INTRODUCTION

In the era of noisy intermediate-scale quantum (NISQ) technology, the practical use of quantum computing is being increasingly pursued, despite challenges like the scarcity of quantum resources and the noise in quantum gates [50]. Key research areas such as combinatorial optimization [21], quantum machine learning [7], and quantum chemistry [41] are recognized as potential fields where NISQ devices might surpass best classical methods, thereby showcasing a quantum advantage.

The Recursive Quantum Approximate Optimization Algorithm (RQAOA) [12] was developed to improve upon the Quantum Approximate Optimization Algorithm (QAOA) for combinatorial optimization problems like maximum cut. While QAOA [21] was initially introduced as a quantum heuristic, research indicates it struggles to surpass the Goemans and Williamson (GW) algorithm [24], a classical method with strong approximation guarantees, at constant depth [5, 20, 31, 39]. In contrast, RQAOA employs a recursive strategy that iteratively refines solutions, demonstrating superior performance both numerically and analytically [2, 11, 13]. This makes RQAOA a promising advancement in quantum optimization.

Research has shown that certain algorithms underperform in specific scenarios, often labeled as hard or worst-case instances [36]. Yet, guidance on how to generate or identify these challenging instances of studies is typically lacking in the literature. For instance, the RQAOA paper highlights an infinite family of d -regular bipartite graphs where the QAOA lags behind the GW algorithm when the depth (number of layers) is $O(\log n)$, where n is the number of nodes [12]. However, the paper does not provide instructions for constructing these graphs. In our work, we seek to bridge this gap by generating instances that underscore the differences between quantum algorithms and classical optimization algorithms in tackling the maximum cut problem, with a particular focus on the RQAOA and GW algorithms. While various heuristics have been explored in [17], we selected the GW algorithm due to its well-established approximation bounds and extensive documentation of both its strengths and limitations, making it a suitable benchmark for comparison. We employ an evolutionary method using the classical Covariance Matrix Adaptation Evolution Strategy (CMA-ES) [28, 30] paired with a fitness function specifically tailored for this purpose. This strategy generates a variety of instances in the latent space of a thoroughly trained Graph Autoencoder (GAE). These instances are designed to be easily solvable by one algorithm

while posing substantial challenges to the other, thereby providing a clearer comparison of their relative strengths and weaknesses.

We deliver several significant contributions:

- We have developed a method that effectively pinpoints maximum cut instances that either pose significant challenges or are considerably more manageable for the RQAOA in comparison to the GW algorithm.
- Through an extensive analysis of these instances across various sizes of the maximum cut problem, our generated instances serve as valuable benchmarks for evaluating and contrasting the effectiveness of different algorithms in addressing maximum cut challenges. This benchmarking not only underscores performance discrepancies among algorithms but also aids in advancing quantum computing methodologies.
- Our research brings a fresh perspective to graph generation studies within the network science community, spurring further investigation and innovation in this domain.

2 PRELIMINARIES

Maximum cut. The maximum cut problem in graphs is one of the classical and well-studied NP-hard combinatorial optimization problems. Given an undirected graph $G = (V, E)$, the goal is to compute a partitioning into two sets $S \subseteq V$ and $V \setminus S$ such that the number of edges

$$C(S) = |\{e \in E \mid e \cap S \neq \emptyset \wedge e \cap (V \setminus S) \neq \emptyset\}|$$

crossing the two sets is maximal. The maximum cut problem is APX-hard [47] and can be approximated using the GW algorithm [24]. Specifically, this approach involves solving a relaxed version of the original problem. We first tackle an optimization problem in the continuous domain $[-1, 1]^N$ using a semidefinite program, which provides us with a real-valued solution associated with a cost denoted as C_{relaxed} . Then, a sampling process, guided by probabilities derived from the entries of the real-valued solution (via a random projection method), is used to produce a feasible solution in the form of a binary string. It is important to note that the cost of the generated binary string is guaranteed to be at most equal to C_{relaxed} , and it is possible that $C_{\text{max}} < C_{\text{relaxed}}$. However, the expected value obtained by the cost function using this method is proven to be less than αC_{max} , where $\alpha \approx 0.878$, for any input graph. In other words, this is an α -approximation algorithm.

The maximum cut problem has received significant attention in the area of quantum optimization and different quantum algorithms have been designed. As discussed earlier, QAOA faces significant limitations due to its intrinsic locality and symmetry constraints, with substantial theoretical research having established no-go theorems in this area. To address these challenges, RQAOA [12] was introduced as an alternative quantum optimization algorithm specifically for combinatorial optimization problems. During each iteration of RQAOA, the problem size—represented as a graph or hypergraph—is reduced by one or more elements, based on correlations between variables derived from QAOA. This reduction process introduces non-local effects by creating new connections between nodes that were not previously linked, thus circumventing the locality constraints of QAOA. Finally, the iterative process stops once

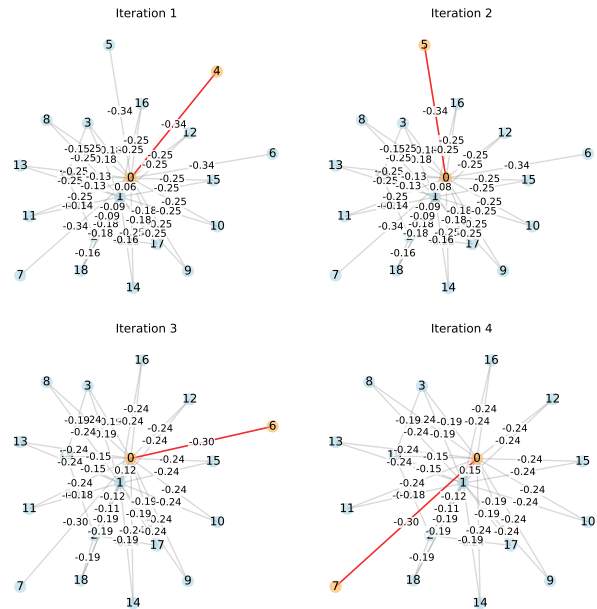


Figure 1: Visualization of RQAOA’s performance ($n_c = 10$) over the first four iterations on a 20-node maximum cut instance, where it outperforms the GW algorithm. Blue dots represent nodes, grey lines indicate edges, and the orange-highlighted node and edge denote the selected operation. The diagram tracks expectation values for each edge at every iteration, with RQAOA choosing the edge with the highest absolute expectation value, selecting randomly in case of a tie.

the number of variables is below a certain predefined threshold n_c ($n_c \approx O(1) \ll |V|$) such that a classical solver can be used to solve the remaining graph. In this study, we focus on depth-1 RQAOA, which can be classically simulated with a runtime of $O(n^4)$ [48]. Understanding the performance of these algorithms is challenging and pointing out instances where quantum approaches perform significantly better or worse than the classical GW algorithm provides an important understanding of their performance in comparison to state-of-the-art classical approximation algorithms.

Figure 1 presents the early performance of the RQAOA (n_c is set to 10) over the first four iterations on a specifically generated 20-node maximum cut instance where it outperforms the GW algorithm. The diagram details the expectation values for each edge during the RQAOA process. In every iteration, the algorithm selects the edge that exhibits the highest absolute expectation value for operation. In cases where several edges possess identical maximum values, one edge is chosen at random. This sequential representation clearly illustrates the strategic process RQAOA employs to make decisions at each step.

Graph Neural Networks (GNNs). GNNs have been proposed to tackle learning problems involving non-Euclidean data [33, 61], among which graph autoencoders (GAEs) are successfully applied to unsupervised tasks to learn graph topologies [35]. GAEs encode

vertices or the entire graph into a latent space, where several different encoding/decoding methods are devised. GAEs have been used to extract network representations and learn the empirical distributions thereof [59]. Due to the famous graph isomorphism issues, the generating/decoding component of GNNs is non-trivial: several works target this issue, including GraphRNN [60] employing a sequential method to construct nodes and edges by learning from a representative set of graphs; GraphVAE [54] that uses variational autoencoders [34] to generate graphs from continuous embeddings.

Covariance Matrix Adaptation Evolution Strategy (CMA-ES). CMA-ES [25, 26] is the state-of-the-art numerical algorithm for black-box optimization problems. CMA-ES employs a set/population of search points, which are sampled from a multivariate Gaussian distribution. CMA-ES selects the subset of points with better objective values and uses their information to update the mean and covariance of the Gaussian. CMA-ES has been successfully applied to various challenging applications and is known for its fast convergence and robustness [9, 29, 37, 52].

3 RELATED WORK

In optimization, generating diverse problem instances is essential for effective benchmarking. The choice of instances significantly impacts algorithm evaluation, making it crucial to update benchmarks regularly to prevent overfitting specific cases. Assessing benchmark quality is challenging, as measuring diversity and representativeness is not straightforward. Typically, evaluation considers key dimensions such as feature space, performance space, and instance space [6].

The literature highlights various methods for generating maximum cut instances used in benchmarking. A notable example is the Balasundarm-Butenko problem generator [3], which utilizes a framework designed for creating test functions within global optimization. This involves applying continuous formulations to combinatorial optimization problems. Another key tool is the machine-independent graph generator known as *Rudy*, introduced by [32] which has been widely used in subsequent research to evaluate algorithms [8, 15, 16]. In 2018, a comprehensive library [17] containing 3,296 diverse instances was introduced, aggregating data from multiple sources, and further enriching the resources available for algorithm testing.

Evolutionary algorithms (EAs) have proven effective in generating diverse problem instances across various domains. Bossek et al. [10] pioneered an EA-based approach for crafting the Travelling Salesperson Problem (TSP) instances using novel mutation operations. Neumann et al. [44] developed a method for evolving diverse TSP instances and images using multi-objective indicators. Gao et al. [22] introduced an EA-driven framework to generate problem instances classified as easy or hard based on distinct features. Addressing diversity in high-dimensional feature spaces, Marrero et al. [38] proposed a Knapsack problem instance generator combining Principal Component Analysis with novelty search. More recently, research has explored evolving instances for the chance-constrained maximum coverage problem [51]. This study departs from traditional approaches that rely on approximation ratios in the (1 + 1) EA, instead incorporating performance ratio variances for improved evaluation.

4 EVOLVING HARD MAXIMUM CUT INSTANCES

GNNs have proven effective for generating graphs with diverse attributes. In our research, we use tools like the GAE to explore and identify specific graph structures. Our goal is to identify hard maximum cut instances. We begin by training a GAE with graph generators that are rooted in network science. After the GAE is adequately trained, we proceed to pinpoint particular graph instances within its complex latent space. The identification process is facilitated by the classical CMA-ES algorithm. This strategy employs a fitness function to assess scenarios where the RQAOA either surpasses or falls short compared to the GW algorithm.

Problem formulation. We aim to propose a method for evolving hard instances of the maximum cut problem, to challenge a recently proposed quantum search algorithm - RQAOA, against a well-studied classical algorithm - GW. We measure the largest number of cuts found by each algorithm on a graph instance I , denoted as $p_{\text{RQAOA}}(I)$, or $p_{\text{GW}}(I)$.

Graph instance representation. We choose to base our research on Permutation-Invariant Variational Autoencoder (PIGVAE) [57] as it handles the graph isomorphism problem explicitly. The core principle of PIGVAE is that identical graphs should yield the same representation, regardless of the order of their nodes. It combines a variational autoencoder with a permuter model. This permuter model, trained in conjunction with the encoder and decoder, assigns a permutation matrix to each input graph. This matrix aligns the node order of the input graph with that of its reconstruction, ensuring consistent representation across different inputs.

Evolving instances with CMA-ES. We aim to search hard graph instances for a maximum cut solver against another solver. Hence, we propose using the following objective function:

$$p_B(I)/p_A(I), \quad (1)$$

where A is the baseline/reference algorithm and B is the one of interest. In this paper, we try to answer two questions: is there a cluster/family of graphs (1) hard to solve by RQAOA w.r.t. the classical GW method; (2) vice versa? For those two questions, we maximize the objective functions, $p_{\text{GW}}(I)/p_{\text{RQAOA}}$ and $p_{\text{RQAOA}}(I)/p_{\text{GW}}$, respectively, in the latent space of the already-trained PIGVAE model. We utilize the widely applied CMA-ES for this maximization task. For each latent point sampled by the CMA-ES, we first decode the latent point to a graph instance I and then execute RQAOA and GW algorithms on instance I 100 times due to their stochasticity. We take the median value of each algorithm to compute the above ratio.

Importantly, a randomly sampled latent point may be decoded into a disconnected graph. We might initiate the CMA-ES with connected graphs. Still, as the search progresses, CMA-ES may sample disconnected graphs again. To resolve this issue, we propose the following strategy: for any latent point that corresponds to a disconnected graph, we solve the maximum cut problems supported on each connected component and then take the sum of the number of cuts from all components. For RQAOA, if the number of nodes of a component is smaller than a preset value n_c , we solve the maximum cut problem on this component by a brute force

method; Otherwise, we apply RQAOA on it. In the recursion step of RQAOA, disconnectedness can be created even if we start with a connected graph. In this case, we apply the above strategy to the connected components. In the experiments, we test our approach with two sizes: 20 nodes and 100 nodes, and we set n_c to 10 and 20, respectively.

5 EXPERIMENTS

5.1 Experimental setup

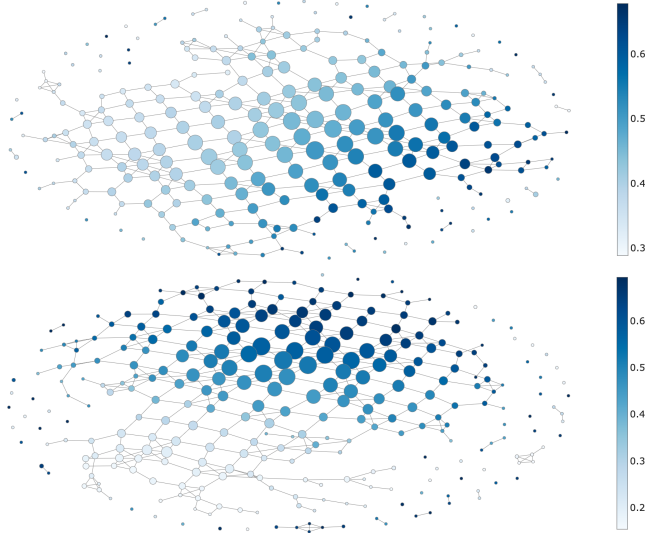


Figure 2: Second-largest eigenvalues of the normalized graph Laplacian for graph embeddings of 20-node (top) and 100-node (bottom) graphs. Nodes represent DBSCAN-identified clusters [19, 53], with edges indicating feature overlap or transitions between clusters. Node colors reflect the second-largest eigenvalue, offering insights into graph connectivity and structural complexity.

GAE training. We sampled the training graph instance u.a.r. from six random graph models: Erdős–Rényi [18], Watts–Strogatz small-world [56], Newman–Watts–Strogatz small-world [45], Random Regular [55], Barabási–Albert [4], and Dual–Barabási–Albert graphs [42]. We also took the parameter setting of those graph models and hyperparameters of the PIGVAE model from [58]. In each training epoch, we generate 6 000 graph instances from the above random models. We train the PIGVAE model with maximally 3 000 epochs and a batch size of 128. An early stopping mechanism is implemented to terminate training if the validation loss shows no improvement over the past 60 epochs. To assess our approach on different graph sizes, we train two separate models: one for 20-node instances and the other for 100-node instances.

CMA-ES setup. The CMA-ES algorithm is configured with a population size of 64, leveraging parallel evaluations to enhance computational efficiency. To further optimize performance, a restart mechanism is implemented, allowing up to 10 restarts, with each

limited to a maximum of 2,000 function evaluations. The algorithm is based on the standard implementation provided by the pycma library [27].

Reproducibility. The full implementation is available in our Zenodo repository [1], along with supplementary materials for reproducibility and reference.

5.2 Results

5.2.1 Evaluation of the GAE. During the training phase, we randomly save 60 graphs out of 6,000 in each epoch, accumulating a total of 6,000 graphs for in-depth evaluation. Our initial examination focuses on the 64-dimensional latent space structure, utilizing embeddings generated from these 6,000 graphs. Initially, we compute several key features, as detailed in Section 7.1 (see the supplementary material [1]), prioritizing those that significantly influence the complexity and difficulty of the maximum cut problem. Research indicates that certain graph characteristics, especially eigenvalues, provide substantial insight into a graph’s connectivity and complexity concerning the maximum cut problem [17, 43]. Figure 2 presents the second-largest eigenvalues of the normalized graph Laplacian for 20-node and 100-node graphs. Nodes represent graph embedding clusters identified via DBSCAN clustering [19, 53], with edges indicating feature overlap or transitions between clusters. Node color reflects the second-largest eigenvalue, revealing graph connectivity and structural complexity. The visualization demonstrates the smooth consistency of embeddings, validating the well-trained GAE’s suitability for generating new graphs for further analysis.

We continue to evaluate our trained GAE through a link prediction task, leveraging learned embeddings to capture graph topology. These embeddings facilitate adjacency matrix reconstruction, enabling predictions of potential node connections. Performance is measured using the macro area under the receiver operating characteristics curve (ROC-AUC) (0 to 1 scale, where 0.5 indicates random guessing and 1 denotes perfect prediction). Our initial assessment focuses on a GAE trained on 10-node Erdős–Rényi graphs (50% probability) using a single A100 GPU with a batch size of 32. This setup yields a macro ROC-AUC of 0.933 ± 0.004 across 6,000 graphs training graphs. Building on this promising result, we extend our analysis to larger graphs containing all graph models, obtaining macro ROC-AUC scores of 0.709 ± 0.001 for 20-node graphs and 0.611 ± 0.001 for 100-node graphs, using the same number of training samples.

5.2.2 Feature analysis through parallel coordinate plot. To ensure diversity, each CMA-ES run begins from different latent points within the latent space. For 20-node maximum cut instances, we generate 1,519 instances where RQAOA outperformed GW and 1,231 instances where GW exceeded the performance of RQAOA. Similarly, for 100-node instances, both algorithms outperform each other in 850 cases. To further analyze these instances, we examine various features (see section 7.1 in the supplementary material [1]). Comparative results are visualized in Figure 3a for 20-node graphs and Figure 3b for 100-node graphs.

Figure 3a presents feature comparisons for maximum cut instances where RQAOA and GW exhibit differing performance. The top subplot highlights cases where RQAOA outperforms GW, with

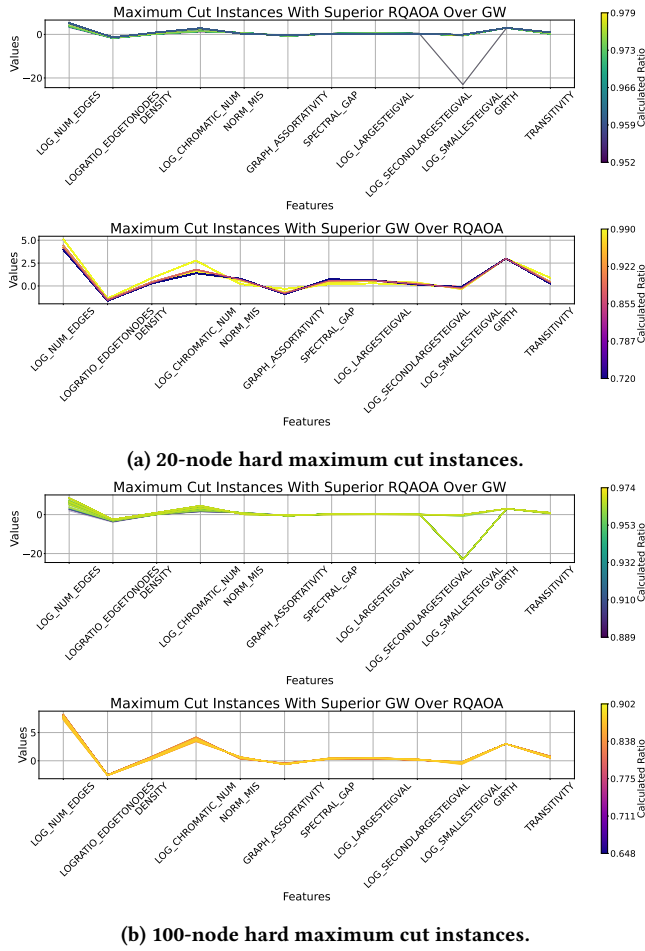


Figure 3: Computed features of generated 20-node (top) and 100-node (bottom) hard maximum cut instances. Each pair of charts highlights cases where either the RQAOA or GW algorithm outperforms the other, with the color bar representing ratio values. Lower values indicate instances where one algorithm significantly outperforms the other.

darker shades indicating greater superiority. The bottom subplot shows instances favoring GW, revealing that lower performance ratios (indicating stronger performance) appear more frequently when GW surpasses RQAOA. RQAOA-dominated instances exhibit a narrow performance ratio range (0.952–0.979), whereas GW-favored cases span a wider range (0.720–0.990). A key distinction emerges in LOG_SMALLESTEIGVAL, where RQAOA-preferred graphs fall below -20, suggesting structural isolation. A representative case, featuring a mostly connected graph with one isolated node, illustrates this trend. Running 100 trials per algorithm on this instance, RQAOA outperforms GW in only 4 trials, with identical results in the rest, implying that GW’s inherent randomness may influence its comparative performance. Figure 3b reveals a similar trend for 100-node graphs, indicating no significant differences in computed features compared to the 20-node case.

Important score	Feature
0.1471 ± 0.0059	EXPECTED_COSTGW_OVER_SDP_COST
0.1370 ± 0.0084	SPECTRAL_GAP
0.0769 ± 0.0057	PERCENT_CLOSE1_LOWER_TRIANGULAR
0.0684 ± 0.0031	PERCENT_POSITIVE_LOWER_TRIANGULAR
0.0665 ± 0.0073	LOG_SECONDLARGESTEIGVAL
0.0528 ± 0.0042	LOG_LARGESTEIGVAL
0.0527 ± 0.0042	DENSITY
0.0521 ± 0.0056	LOG_NUM_EDGES
0.0508 ± 0.0051	PERCENT_CLOSE3_LOWER_TRIANGULAR
0.0434 ± 0.0068	LOGRATIO_EDGETONODES
0.0431 ± 0.0040	NORM_MIS
0.0413 ± 0.0036	GRAPH_ASSORTATIVITY
0.0408 ± 0.0042	TRANSITIVITY
0.0378 ± 0.0027	STD_COSTGW_OVER_SDP_COST
0.0369 ± 0.0049	PERCENT_CUT
0.0310 ± 0.0052	LOG_SMALLESTEIGVAL
0.0215 ± 0.0041	LOG_CHROMATIC_NUM
0.0000 ± 0.0000	GIRTH

Table 1: Important features with the classifier built on 20-node maximum cut instances.

Important score	Feature
0.3749 ± 0.0104	EXPECTED_COSTGW_OVER_SDP_COST
0.1588 ± 0.0196	LOG_SMALLESTEIGVAL
0.1281 ± 0.0052	PERCENT_CLOSE1_LOWER_TRIANGULAR
0.0648 ± 0.0081	PERCENT_CUT
0.0618 ± 0.0049	PERCENT_CLOSE3_LOWER_TRIANGULAR
0.0454 ± 0.0071	DENSITY
0.0322 ± 0.0054	GRAPH_ASSORTATIVITY
0.0239 ± 0.0049	LOG_LARGESTEIGVAL
0.0199 ± 0.0085	LOG_NUM_EDGES
0.0165 ± 0.0037	NORM_MIS
0.0153 ± 0.0036	TRANSITIVITY
0.0143 ± 0.0026	LOG_SECONDLARGESTEIGVAL
0.0126 ± 0.0061	LOGRATIO_EDGETONODES
0.0116 ± 0.0026	LOG_CHROMATIC_NUM
0.0096 ± 0.0030	SPECTRAL_GAP
0.0061 ± 0.0032	PERCENT_POSITIVE_LOWER_TRIANGULAR
0.0043 ± 0.0025	STD_COSTGW_OVER_SDP_COST
0.0000 ± 0.0000	GIRTH

Table 2: Important features with the classifier built on 100-node maximum cut instances.

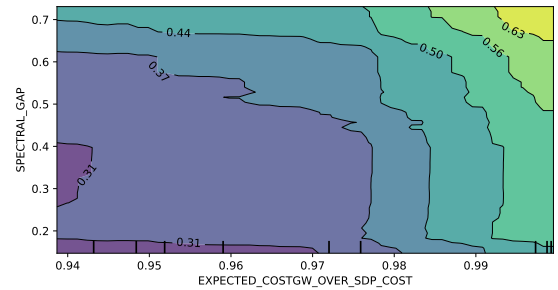
5.2.3 Feature analysis with machine learning pipeline. To analyze the GW algorithm’s role in generating hard maximum cut instances, we expand our feature set based on prior research [43]. Incorporating six additional GW-related features (see Section 7.2 in the supplementary material [1]), we increase our total to 18 features within our machine learning pipeline. NP-hard features like the domination number are considered but excluded due to their computational complexity and minimal impact on model accuracy. For classification, we use the TPOP library [46], an AutoML tool for optimizing machine learning pipelines. Instances, where RQAOA

outperforms GW, are labeled 0, while GW-dominant cases are labeled 1. We split the dataset 70:30 for training and testing. Due to class imbalance, particularly in 20-node experiments, we optimize for balanced accuracy [14], while standard accuracy [49] is used for the balanced 100-node dataset. Using TPOP, we conduct 10-fold cross-validation over 100 generations, evaluating 60 candidate solutions per generation.

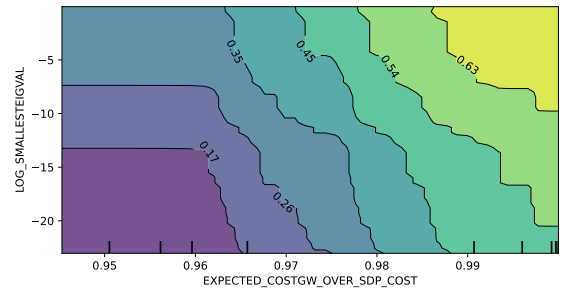
In our 20-node experiments, we achieve an outstanding average balanced accuracy of 0.9988 ± 0.0012 across ten runs, each with a unique random data split. This result is obtained using an ExtraTreesClassifier [23] (parameters detailed in section 7.3). Key predictive features include EXPECTED_COSTGW_OVER_SDP_COST and SPECTRAL_GAP, where the former evaluates GW’s effectiveness, and the latter reflects graph spectral properties as shown in Table 1. The relevance of the GW algorithm’s output in our analysis aligns with our focus on instances that are particularly challenging for maximum cut problems, influenced by the GW performance. The importance of eigenvalues also plays a crucial role, as seen in LOG_SECOND LARGESTEIGVAL and LOG_LARGESTEIGVAL, while GIRTH (shortest cycle length) contributes little to classifier performance. Further, the partial dependence plot visualizes the impact of two top features as shown in Figure 4a. This plot demonstrates how these features influence the probability of predicting class 1, which in this study corresponds to instances where GW outperforms RQAOA. The plot reveals a clear trend: as the feature value changes, the probability of an instance being classified as class 1 increases, indicating a positive correlation between these features and the probability of challenging GW.

In the analysis of 100-node instances, we achieve perfect accuracy, recorded as 1.0000 ± 0.0000 , using an ExtraTreesClassifier. The parameters for this classifier are outlined in section 7.3. As indicated in Table 2, the feature EXPECTED_COSTGW_OVER_SDP_COST stands out as the most significant, showing a much higher influence compared to other features. This finding is in line with our earlier results from the 20-node experiments, where four out of the five most influential features are similarly linked to the performance metrics of the GW algorithm. Consistent with previous observations, the feature GIRTH, which do not impact the classifier’s decisions. The influence of the primary features is visualized in Figure 4b through a partial dependence plot. It illustrates that as the values of EXPECTED_COSTGW_OVER_SDP_COST and LOG_SMALLESTEIGVAL increase, there is a corresponding rise in the probability that an instance will perform better under GW compared to RQAOA.

To assess the significance of features, we conduct a permutation important analysis. This involved randomly shuffling the values within columns of our dataset, focusing particularly on the top two features identified in both the 20-node and 100-node experiments. For each feature, we generate 10 different permutations of our original dataset. We then evaluate the impact of these permutations on the model’s performance, which is initially trained on the unaltered dataset, using the same 10 seeds as the original setup. For the 20-node experiments, the permutation of the feature EXPECTED_COSTGW_OVER_SDP_COST results in a slight decrease in performance, with metrics changing by a -0.0006 ± 0.0018 . Interestingly, shuffling the SPECTRAL_GAP feature leads to a minor performance increase, indicated by 0.0001 ± 0.0017 . When both features



(a) Partial dependence plot showing the impact of the top two features on 20-node maximum cut instances.

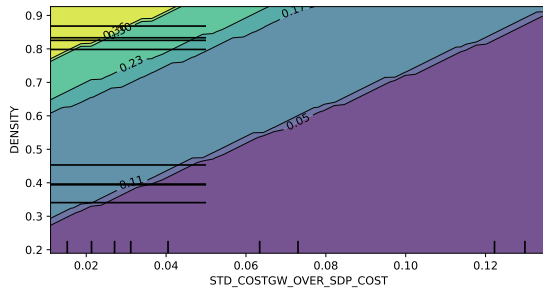


(b) Partial dependence plot showing the impact of the top two features on 100-node maximum cut instances.

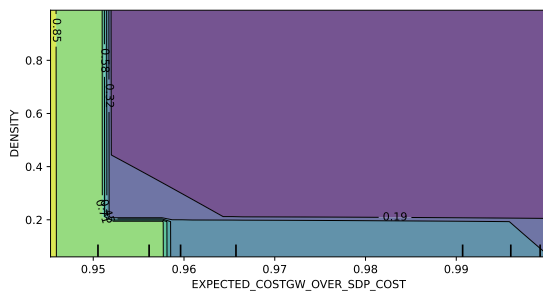
Figure 4: Partial dependence plots showing the classifier’s response to the top two features of 20-node (top) and 100-node (bottom) maximum cut instances. The contour lines represent different probability levels, providing insight into feature influence.

are permuted simultaneously, the combined effect causes a more noticeable performance decrease of 0.0009 ± 0.00177 . In the 100-node experiments, permutating the EXPECTED_COSTGW_OVER_SDP_COST feature lead to a more pronounced decline in performance, measured at -0.0067 ± 0.0048 . Permutation of the feature LOG_SMALLESTEIGVAL results in a smaller drop in performance, recorded as -0.0004 ± 0.0008 on performance due to the. Permutating both features together causes a decrease in performance of -0.0012 ± 0.0013 . Overall, we can conclude that the performance shifts upon permutating a single feature or two top features slightly affect the model’s performance.

To determine whether classifier performance could be sustained without the top two most informative features identified in our 20-node and 100-node experiments, we re-initiate the entire automated machine learning process excluding these features. In the 20-node experiments, this exclusion results in a minor decrease in performance, showing a decline of 0.0015 ± 0.0022 from the original baseline. Interestingly, in the 100-node experiments, performance remained unchanged, suggesting that the other features in the dataset still carry significant predictive power and are capable of compensating for the absence of the top two features. As indicated



(a) Partial dependence plot highlighting key features that distinguish significant RQAOA performance gains on 20-node maximum cut instances, based on permutation importance.



(b) Partial dependence plot highlighting key features that distinguish significant RQAOA performance gains on 100-node maximum cut instances, based on permutation importance.

Figure 5: Partial dependence plots illustrating the classifier’s behavior in identifying significant performance gains with RQAOA for 20-node (top) and 100-node (bottom) maximum cut instances. The plots highlight the influence of the top two features in distinguishing performance improvements, as determined by permutation importance.

in the study [43], two features associated with GW performance are identified as the most significant factors for building the classifiers. Motivated to further explore this, we test whether classifiers built solely on GW-related features could maintain similar levels of performance. The results show a substantial drop in the 20-node experiment with accuracy falling to 0.9250 ± 0.1541 , indicating that GW-related features alone are not sufficient at this scale. However, the 100-node experiment continues to achieve perfect accuracy of 1.0000 ± 0.0000 . These findings suggest that while the GW-related features are insufficient on their own for the 20-node experiments, they provide substantial support in building the classifier with our 100-node instances.

5.2.4 RQAOA as a high-performing heuristic with machine learning pipeline. After successfully applying our evolutionary approach to evolve hard maximum cut instances, a new question emerges: whether RQAOA consistently performs well? For our purposes, we seek to establish if RQAOA can achieve a performance level above 0.96, with a minimum advantage of 0.04 over the GW algorithm. In

Important score	Feature
0.0665 ± 0.0641	STD_COSTGW_OVER_SDP_COST
0.0361 ± 0.0382	DENSITY
0.0355 ± 0.0389	NORM_MIS
0.0352 ± 0.0383	GRAPH_ASSORTATIVITY
0.0347 ± 0.0372	LOG_LARGESTEIGVAL
0.0345 ± 0.0376	LOG_CHROMATIC_NUM
0.0331 ± 0.0344	TRANSITIVITY
0.0319 ± 0.0201	SPECTRAL_GAP
0.0180 ± 0.0191	LOG_SECONDLARGESTEIGVAL
0.0082 ± 0.0051	LOG_SMALLESTEIGVAL
0.0031 ± 0.0034	PERCENT_POSITIVE_LOWER_TRIANGULAR
0.0031 ± 0.0039	LOG_NUM_EDGES
0.0028 ± 0.0049	PERCENT_CUT
0.0012 ± 0.0025	LOGRATIO_EDGETONODES
0.0010 ± 0.0048	PERCENT_CLOSE1_LOWER_TRIANGULAR
0.0002 ± 0.0051	PERCENT_CLOSE3_LOWER_TRIANGULAR
0.0000 ± 0.0000	GIRTH
-0.0002 ± 0.0029	EXPECTED_COSTGW_OVER_SDP_COST

Table 3: Important features with the classifier built on 20-node maximum cut instances demonstrate RQAOA’s high performance, underscored by its significant permutation importance.

Important score	Feature
0.0243 ± 0.0379	EXPECTED_COSTGW_OVER_SDP_COST
0.0166 ± 0.0339	DENSITY
0.0114 ± 0.0057	LOGRATIO_EDGETONODES
0.0066 ± 0.0110	NORM_MIS
0.0036 ± 0.0106	LOG_SECONDLARGESTEIGVAL
0.0028 ± 0.0047	LOG_NUM_EDGES
0.0023 ± 0.0048	LOG_LARGESTEIGVAL
0.0011 ± 0.0020	PERCENT_POSITIVE_LOWER_TRIANGULAR
0.0010 ± 0.0052	LOG_CHROMATIC_NUM
0.0003 ± 0.0027	STD_COSTGW_OVER_SDP_COST
0.0003 ± 0.0004	SPECTRAL_GAP
0.0001 ± 0.0002	TRANSITIVITY
0.0000 ± 0.0000	GIRTH
-0.0001 ± 0.0004	PERCENT_CLOSE1_LOWER_TRIANGULAR
-0.0001 ± 0.0003	PERCENT_CLOSE3_LOWER_TRIANGULAR
-0.0002 ± 0.0004	PERCENT_CUT
-0.0002 ± 0.0008	GRAPH_ASSORTATIVITY
-0.0153 ± 0.0118	LOG_SMALLESTEIGVAL

Table 4: Important features with the classifier built on 100-node maximum cut instances demonstrate RQAOA’s high performance, underscored by its significant permutation importance.

this study, we reassess the same dataset with a modified labelling strategy. Instances are labelled as 1 when the ratio of GW to RQAOA is 0.96 or less, indicating at least a 4% improvement over the GW algorithm. All other instances are labelled as 0. We develop classifiers on both 20-node and 100-node instances that incorporate all the features previously discussed with achieved a balanced accuracy

of 0.9826 ± 0.0042 on 20-node experiments and a 0.8343 ± 0.0303 in the 100-node experiment, maintaining the same experimental and analysis procedures as before. The models, generated using the TPOP library are detailed further in section 7.3. Figure 5 shows the partial dependent plot for the top two features in both 20-node and 100-node cases, respectively. The calculation of feature importance scores is based on permutation importance [49]. The analysis of these plots reveals a clear pattern: low values in GW-related features are strongly associated with increased predicted probabilities of RQAOA achieving outstanding performance. Moreover, the significance of the DENSITY feature in influencing RQAOA's performance is evident. This analysis not only shows the impact of GW-related cost features but also emphasizes the critical role of DENSITY in determining the effectiveness of the RQAOA algorithm.

Table 3 and Table 4 showcase the key features identified by the classifier for 20-node and 100-node maximum cut instances, respectively. Highlighted in these tables, the features emphasize the robust performance of RQAOA, validating its effectiveness as a high-performing heuristic through significant permutation importance.

We evaluate the performance of RQAOA against different thresholds to better understand our generated instances. Initially, thresholds of 0.95 and 0.98 are also considered; however, they are discarded because there are different situations related to 20-node or 100-node instances that no instances meet the criteria to be labelled as 1. At a threshold of 0.97, the average balanced accuracy achieved is 0.9795 ± 0.0045 for 20-node instances, which is comparable to the performance at a threshold of 0.96. LOG_CHROMATIC_NUM and GRAPH_ASSORTATIVITY are identified as the most significant features according to permutation importance calculations. For 100-node instances, the performance improved notably at the 0.97 threshold, achieving an average balanced accuracy of 0.9214 ± 0.0049 . This represents a substantial enhancement over the results obtained with the 0.96 threshold. The most influential features for this larger node size are identified as PERCENT_CLOSE3_LOWER_TRIANGULAR and GRAPH_ASSORTATIVITY. These results demonstrate that the model's effectiveness varies significantly with different threshold settings, with each threshold providing unique insights, especially in scenarios involving larger graph instances. This responsiveness underscores the need to thoughtfully choose performance benchmarks that align with the unique attributes and requirements of the dataset.

6 CONCLUSION

Given the current literature does not provide detailed guidelines for constructing hard maximum cut instances, our research aims to address this gap. We focus on developing instances that highlight the distinctions between the quantum method RQAOA and the classical GW algorithm by effectively identifying maximum cut instances that pose significant challenges or are notably manageable for the RQAOA compared to the performance of the GW algorithm. Specifically, our work extends beyond situations where RQAOA merely surpasses GW, exploring instances where RQAOA achieves exceptionally high-quality outcomes and significantly outperforms GW. We employ an evolutionary approach using the classical CMA-ES algorithm, enhanced with a fitness function specifically tailored within the latent space of a well-trained Graph Autoencoder.

Drawing on precedents that applied machine learning to analyze the performance of quantum methods [40, 43], we adapt a comprehensive machine-learning pipeline. This approach examines a wide array of features, from those common to regular graphs and the spectrum of the Laplacian matrix to those associated with the relaxed solution of the semi-definite program in GW. Our feature analysis of the generated instances has further substantiated that RQAOA can offer substantial benefits over the GW algorithm.

In predicting these advantages, the machine learning model we developed strong results across both 20-node and 100-node instances. It confirms the necessity of both categories of features in analyzing instances where RQAOA significantly outperforms GW, reinforcing the comprehensive nature of the analytical framework. Our findings highlight EXPECTED_COSTGW_OVER_SDP_COST as the most influential feature when RQAOA is not considered a high-performing heuristic. This trend remains consistent in 100-node maximum cut instances when we consider RQAOA as a high-performing heuristic but does not hold for 20-node instances. Conversely, DENSITY plays a key role when RQAOA functions as a high-performing heuristic. Beyond these primary features, various other features also contribute to the machine learning classifiers, but GIRTH is found to have no impact in either experimental setting.

Our study offers a fresh perspective on graph generation within network science, encouraging further exploration and advancements in this area. Future work can be explored from various perspectives. Our current experiments focus on graphs with 20 and 100 nodes, but we are actively working to scale up to larger instances, such as 400-node graphs. A major challenge in this expansion is the scalability of the PIGVAE model, which was originally developed for smaller graphs and faces significant memory constraints when applied to larger ones. Running the model on 400-node graphs leads to severe computational bottlenecks. To address this, we have reduced the model's size, but this comes at the potential cost of training performance. Moving forward, we aim to explore alternative strategies to improve scalability, enabling the model to efficiently process graphs with thousands of nodes while maintaining its effectiveness. Additionally, as part of our future work, we aim to integrate additional heuristics beyond GW to enhance the depth of our comparative analysis.

REFERENCES

- [1] Anonymous Authors(s). 2025. Evolving Hard Maximum Cut Instances for Quantum Approximate Optimization Algorithms: Supplementary Material. <https://doi.org/10.5281/zenodo.14757740>.
- [2] Eunok Bae and Soojoon Lee. 2024. Recursive QAOA outperforms the original QAOA for the MAX-CUT problem on complete graphs. *Quantum Information Processing* 23, 3 (2024), 78.
- [3] Balabhaskar Balasundaram and Sergiy Butenko. 2005. Constructing test functions for global optimization using continuous formulations of graph problems. *Optimization Methods and Software* 20, 4-5 (2005), 439–452.
- [4] Albert-László Barabási and Réka Albert. 1999. Emergence of scaling in random networks. *science* 286, 5439 (1999), 509–512.
- [5] Boaz Barak and Kunal Marwaha. 2022. Classical Algorithms and Quantum Limitations for Maximum Cut on High-Girth Graphs. In *13th Innovations in Theoretical Computer Science Conference, ITCS 2022 (LIPIcs, Vol. 215)*. Schloss Dagstuhl - Leibniz-Zentrum für Informatik, 14:1–14:21.
- [6] Thomas Bartz-Beielstein, Carola Doerr, Daan van den Berg, Jakob Bossek, Sowmya Chandrasekaran, Tome Eftimov, Andreas Fischbach, Pascal Kerschke, William La Cava, Manuel Lopez-Ibanez, et al. 2020. Benchmarking in optimization: Best practice and open issues. *arXiv preprint arXiv:2007.03488* (2020).
- [7] Marcello Benedetti, Erika Lloyd, Stefan Sack, and Mattia Fiorentini. 2019. Parameterized quantum circuits as machine learning models. *Quantum Science and*

- Technology 4, 4 (2019), 043001.
- [8] Steven J Benson, Yinyu Yeb, and Xiong Zhang. 1999. Mixed linear and semidefinite programming for combinatorial and quadratic optimization. *Optimization Methods and Software* 11, 1-4 (1999), 515–544.
 - [9] Xavier Bonet-Monroig, Hao Wang, Diederick Vermetten, Bruno Senjean, Charles Moussa, Thomas Bäck, Vedran Dunjko, and Thomas E O'Brien. 2023. Performance comparison of optimization methods on variational quantum algorithms. *Physical Review A* 107, 3 (2023), 032407.
 - [10] Jakob Bossek, Pascal Kerschke, Aneta Neumann, Markus Wagner, Frank Neumann, and Heike Trautmann. 2019. Evolving diverse TSP instances by means of novel and creative mutation operators. In *Proceedings of the 15th ACM/SIGEVO conference on foundations of genetic algorithms*. 58–71.
 - [11] Sergey Bravyi, David Gosset, and Daniel Grier. 2021. Classical algorithms for Forrelation. *arXiv preprint arXiv:2102.06963* (2021).
 - [12] Sergey Bravyi, Alexander Kliesch, Robert Koenig, and Eugene Tang. 2020. Obstacles to variational quantum optimization from symmetry protection. *Physical review letters* 125, 26 (2020), 260505.
 - [13] Sergey Bravyi, Alexander Kliesch, Robert Koenig, and Eugene Tang. 2022. Hybrid quantum-classical algorithms for approximate graph coloring. *Quantum* 6 (2022), 678.
 - [14] Kay Henning Brodersen, Cheng Soon Ong, Klaas Enno Stephan, and Joachim M. Buhmann. 2010. The Balanced Accuracy and Its Posterior Distribution. In *20th International Conference on Pattern Recognition, ICPR 2010*. IEEE Computer Society, 3121–3124. doi:10.1109/ICPR.2010.764
 - [15] Samuel Burer and Renato DC Monteiro. 2001. A projected gradient algorithm for solving the maxcut SDP relaxation. *Optimization methods and Software* 15, 3-4 (2001), 175–200.
 - [16] Samuel Burer, Renato DC Monteiro, and Yin Zhang. 2002. Rank-two relaxation heuristics for max-cut and other binary quadratic programs. *SIAM Journal on Optimization* 12, 2 (2002), 503–521.
 - [17] Iain Dunning, Swati Gupta, and John Silberholz. 2018. What works best when? A systematic evaluation of heuristics for Max-Cut and QUBO. *INFORMS Journal on Computing* 30, 3 (2018), 608–624.
 - [18] Paul Erdos and Alfréd Rényi. 1960. On the evolution of random graphs. *Publ. Math. Inst. Hungar. Acad. Sci* 5 (1960), 17–61.
 - [19] Martin Ester, Hans-Peter Kriegel, Jörg Sander, Xiaowei Xu, et al. 1996. A density-based algorithm for discovering clusters in large spatial databases with noise. In *KDD*, Vol. 96. 226–231.
 - [20] Edward Farhi, David Gamarnik, and Sam Gutmann. 2020. The quantum approximate optimization algorithm needs to see the whole graph: A typical case. *arXiv preprint arXiv:2004.09002* (2020).
 - [21] Edward Farhi, Jeffrey Goldstone, and Sam Gutmann. 2014. A quantum approximate optimization algorithm. *arXiv preprint arXiv:1411.4028* (2014).
 - [22] Wanru Gao, Samadhi Nallaperuma, and Frank Neumann. 2021. Feature-based diversity optimization for problem instance classification. *Evolutionary Computation* 29, 1 (2021), 107–128.
 - [23] Pierre Geurts, Damien Ernst, and Louis Wehenkel. 2006. Extremely randomized trees. *Mach. Learn.* 63, 1 (2006), 3–42. doi:10.1007/S10994-006-6226-1
 - [24] Michel X Goemans and David P Williamson. 1995. Improved approximation algorithms for maximum cut and satisfiability problems using semidefinite programming. *Journal of the ACM (JACM)* 42, 6 (1995), 1115–1145.
 - [25] Nikolaus Hansen. 2006. The CMA Evolution Strategy: A Comparing Review. In *Towards a New Evolutionary Computation - Advances in the Estimation of Distribution Algorithms*. Studies in Fuzziness and Soft Computing, Vol. 192. Springer, 75–102. doi:10.1007/3-540-32494-1_4
 - [26] Nikolaus Hansen. 2016. The CMA Evolution Strategy: A Tutorial. *CoRR abs/1604.00772* (2016). arXiv:1604.00772 <http://arxiv.org/abs/1604.00772>
 - [27] Nikolaus Hansen, Youhei Akimoto, and Petr Baudis. 2019. CMA-ES/pycma on Github. Zenodo, DOI:10.5281/zenodo.2559634. doi:10.5281/zenodo.2559634
 - [28] Nikolaus Hansen, Sibylle D Müller, and Petros Koumoutsakos. 2003. Reducing the time complexity of the derandomized evolution strategy with covariance matrix adaptation (CMA-ES). *Evolutionary computation* 11, 1 (2003), 1–18.
 - [29] Nikolaus Hansen, André S. P. Niederberger, Lino Guzzella, and Petros Koumoutsakos. 2009. A Method for Handling Uncertainty in Evolutionary Optimization With an Application to Feedback Control of Combustion. *IEEE Trans. Evol. Comput.* 13, 1 (2009), 180–197. doi:10.1109/TEVC.2008.924423
 - [30] Nikolaus Hansen and Andreas Ostermeier. 2001. Completely derandomized self-adaptation in evolution strategies. *Evolutionary computation* 9, 2 (2001), 159–195.
 - [31] Matthew B. Hastings. 2019. Classical and quantum bounded depth approximation algorithms. *Quantum Inf. Comput.* 19, 13&14 (2019), 1116–1140. doi:10.26421/QIC19.13-14-3
 - [32] Christoph Helmberg and Franz Rendl. 2000. A spectral bundle method for semidefinite programming. *SIAM Journal on Optimization* 10, 3 (2000), 673–696.
 - [33] Wei Ju, Siyu Yi, Yifan Wang, Zhiping Xiao, Zhengyang Mao, Hourun Li, Yiyang Gu, Yifang Qin, Nan Yin, Senzhang Wang, Xinwang Liu, Xiao Luo, Philip S. Yu, and Ming Zhang. 2024. A Survey of Graph Neural Networks in Real World: Imbalance, Noise, Privacy and OOD Challenges. *CoRR abs/2403.04468* (2024). doi:10.48550/ARXIV.2403.04468 arXiv:2403.04468
 - [34] Diederik P. Kingma and Max Welling. 2014. Auto-Encoding Variational Bayes. In *2nd International Conference on Learning Representations, ICLR 2014*. <http://arxiv.org/abs/1312.6114>
 - [35] Thomas N. Kipf and Max Welling. 2016. Variational Graph Auto-Encoders. *CoRR abs/1611.07308* (2016). <https://dblp.org/rec/journals/corr/KipfW16a>
 - [36] Ker-I Ko, Pekka Orponen, Uwe Schöning, and Osamu Watanabe. 1986. What is a hard instance of a computational problem?. In *Structure in Complexity Theory: Proceedings of the Conference held at the University of California, Berkeley, California, June 2–5, 1986*. Springer, 197–217.
 - [37] Ilya Loshchilov and Frank Hutter. 2016. CMA-ES for Hyperparameter Optimization of Deep Neural Networks. *CoRR abs/1604.07269* (2016). arXiv:1604.07269 <http://arxiv.org/abs/1604.07269>
 - [38] Alejandro Marrero, Eduardo Segredo, Emma Hart, Jakob Bossek, and Aneta Neumann. 2023. Generating diverse and discriminatory knapsack instances by searching for novelty in variable dimensions of feature-space. In *Proceedings of the Genetic and Evolutionary Computation Conference, GECCO 2023*. ACM, 312–320.
 - [39] Kunal Marwaha. 2021. Local classical MAX-CUT algorithm outperforms $p = 2$ QAOA on high-girth regular graphs. *Quantum* 5 (2021), 437.
 - [40] Alexey A Melnikov, Leonid E Fedichkin, and Alexander Alodjants. 2019. Predicting quantum advantage by quantum walk with convolutional neural networks. *New Journal of Physics* 21, 12 (2019), 125002.
 - [41] Nikolaj Moll, Panagiotis Barkoutsos, Lev S Bishop, Jerry M Chow, Andrew Cross, Daniel J Egger, Stefan Filipp, Andreas Fuhrer, Jay M Gambetta, Marc Ganzhorn, et al. 2018. Quantum optimization using variational algorithms on near-term quantum devices. *Quantum Science and Technology* 3, 3 (2018), 030503.
 - [42] Niema Moshiri. 2018. The dual-Barabási-Albert model. *arXiv preprint arXiv:1810.10538* (2018).
 - [43] Charles Moussa, Henri Calandra, and Vedran Dunjko. 2020. To quantum or not to quantum: towards algorithm selection in near-term quantum optimization. *Quantum Science and Technology* 5, 4 (2020), 044009.
 - [44] Aneta Neumann, Wanru Gao, Markus Wagner, and Frank Neumann. 2019. Evolutionary diversity optimization using multi-objective indicators. In *Proceedings of the Genetic and Evolutionary Computation Conference, GECCO 2019*. ACM, 837–845. doi:10.1145/3321707.3321796
 - [45] Mark EJ Newman and Duncan J Watts. 1999. Renormalization group analysis of the small-world network model. *Physics Letters A* 263, 4-6 (1999), 341–346.
 - [46] Randal S. Olson, Nathan Bartley, Ryan J. Urbanowicz, and Jason H. Moore. 2016. Evaluation of a Tree-based Pipeline Optimization Tool for Automating Data Science. In *Proceedings of the 2016 on Genetic and Evolutionary Computation Conference*. ACM, 485–492. doi:10.1145/2908812.2908918
 - [47] Christos H. Papadimitriou and Mihalis Yannakakis. 1991. Optimization, Approximation, and Complexity Classes. *J. Comput. Syst. Sci.* 43, 3 (1991), 425–440.
 - [48] Yash J Patel, Sofiene Jerbi, Thomas Bäck, and Vedran Dunjko. 2024. Reinforcement learning assisted recursive QAOA. *EPJ Quantum Technology* 11, 1 (2024), 6.
 - [49] F. Pedregosa, G. Varoquaux, A. Gramfort, V. Michel, B. Thirion, O. Grisel, M. Blondel, P. Prettenhofer, R. Weiss, V. Dubourg, J. Vanderplas, A. Passos, D. Cournapeau, M. Brucher, M. Perrot, and E. Duchesnay. 2011. Scikit-learn: Machine Learning in Python. *Journal of Machine Learning Research* 12 (2011), 2825–2830.
 - [50] John Preskill. 2018. Quantum computing in the NISQ era and beyond. *Quantum* 2 (2018), 79.
 - [51] Saba Sadeghi Ahouei, Jacob De Nobel, Aneta Neumann, Thomas Bäck, and Frank Neumann. 2024. Evolving Reliable Differentiating Constraints for the Chance-constrained Maximum Coverage Problem. In *Proceedings of the Genetic and Evolutionary Computation Conference*. ACM, 1036–1044.
 - [52] Tim Salimans, Jonathan Ho, Xi Chen, and Ilya Sutskever. 2017. Evolution Strategies as a Scalable Alternative to Reinforcement Learning. *CoRR abs/1703.03864* (2017). arXiv:1703.03864 <http://arxiv.org/abs/1703.03864>
 - [53] Erich Schubert, Jörg Sander, Martin Ester, Hans Peter Kriegel, and Xiaowei Xu. 2017. DBSCAN revisited, revisited: why and how you should (still) use DBSCAN. *ACM Transactions on Database Systems (TODS)* 42, 3 (2017), 1–21.
 - [54] Martin Simonovsky and Nikos Komodakis. 2018. Graphvae: Towards generation of small graphs using variational autoencoders. In *Artificial Neural Networks and Machine Learning—ICANN 2018: 27th International Conference on Artificial Neural Networks, Proceedings, Part I 27*. Springer, 412–422.
 - [55] Angelika Steger and Nicholas C Wormald. 1999. Generating random regular graphs quickly. *Combinatorics, Probability and Computing* 8, 4 (1999), 377–396.
 - [56] Duncan J Watts and Steven H Strogatz. 1998. Collective dynamics of 'small-world' networks. *Nature* 393, 6684 (1998), 440–442.
 - [57] Robin Winter, Frank Noé, and Djork-Arné Clevert. 2021. Permutation-Invariant Variational Autoencoder for Graph-Level Representation Learning. In *Advances in Neural Information Processing Systems 34: Annual Conference on Neural Information Processing Systems 2021, NeurIPS 2021*. 9559–9573. <https://proceedings.neurips.cc/paper/2021/hash/4f3d7d38d24b740c95da2b03dc3a2333-Abstract.html>
 - [58] Robin Winter, Frank Noé, and Djork-Arné Clevert. 2021. Permutation-invariant variational autoencoder for graph-level representation learning. *Advances in Neural Information Processing Systems* 34 (2021), 9559–9573.

- [59] Zonghan Wu, Shirui Pan, Fengwen Chen, Guodong Long, Chengqi Zhang, and S Yu Philip. 2020. A comprehensive survey on graph neural networks. *IEEE transactions on neural networks and learning systems* 32, 1 (2020), 4–24.
- [60] Jiaxuan You, Rex Ying, Xiang Ren, William Hamilton, and Jure Leskovec. 2018. GraphRNN: Generating realistic graphs with deep auto-regressive models. In *International conference on machine learning*. PMLR, 5708–5717.
- [61] Yanqiao Zhu, Yuanqi Du, Yinkai Wang, Yichen Xu, Jieyu Zhang, Qiang Liu, and Shu Wu. 2022. A survey on deep graph generation: Methods and applications. In *Learning on Graphs Conference*. PMLR, 47–1.

7 APPENDIX

7.1 Appendix A

The features of the instances utilized in this study are detailed as follows:

- **LOG_NUM_EDGES**: The logarithm of the number of edges in the graph.
- **DENSITY**: The proportion of actual edges to the maximum possible number of edges (i.e., of a complete graph).
- **LOGRATIO_EDGETONODES**: The natural logarithm of the edge-to-node ratio.
- **LOG_CHROMATIC_NUM**: The logarithm of the minimum number of colours required to colour the graph such that no two adjacent nodes share the same colour.
- **NORM_MIS**: The size of the largest independent node-set, adjusted relative to the total number of nodes, showcasing the proportion of non-adjacent nodes.
- **GRAPH_ASSORTATIVITY**: Gauges node connection similarity based on node degree, with values near 1 suggesting similar degree connections.
- **SPECTRAL_GAP**: The difference between the largest and second-largest eigenvalues of the graph's normalized Laplacian matrix.
- **LOG_LARGESTEIGVAL**: The logarithm of the highest eigenvalue from the normalized Laplacian matrix.
- **LOG_SECONDLARGESTEIGVAL**: The logarithm of the normalized Laplacian matrix's second-largest eigenvalue.
- **LOG_SMALLESTEIGVAL**: The logarithm of the smallest non-trivial eigenvalue from the normalized Laplacian matrix.
- **GIRTH**: The length of the shortest loop in the graph.
- **TRANSITIVITY**: The likelihood ratio of nodes to form tightly connected clusters.

7.2 Appendix B

The features related to the GW algorithm are introduced as follows:

- **PERCENT_CUT**: The ratio of the optimal cut value derived from the semidefinite programming (SDP) solution to the overall number of edges in the graph.
- **PERCENT_POSITIVE_LOWER_TRIANGULAR**: Quantifies the share of positive entries in the lower triangular section of the factorized matrix.
- **PERCENT_CLOSE1_LOWER_TRIANGULAR**: The proportion of elements in the lower triangular of the factorized matrix that have absolute values under 0.1.
- **PERCENT_CLOSE3_LOWER_TRIANGULAR**: The percentage of elements in the lower triangular of the factorized matrix with absolute values smaller than 0.001.
- **EXPECTED_COSTGW_OVER_SDP_COST**: The proportion of the GW approach's average cost (over 1,000 random trials) relative to the maximum theoretical cost as determined by the SDP method.
- **STD_COSTGW_OVER_SDP_COST**: Quantifies the standard deviation of the outcomes from 1,000 random implementations of GW, normalized by the best possible cost determined through the SDP method.

7.3 Appendix C

The models with hyperparameters constructed in the section of feature analysis with machine learning pipeline are highlighted in the following:

- The classifier developed using TPOP for instances involving 20 nodes uses an ExtraTreesClassifier, which comprises a collection of 100 decision trees. This ensemble employs the entropy criterion to determine the quality of splits within the trees. Each tree considers approximately 35% of the features for node splitting. It also ensures that each leaf node has at least one sample, while at least nine samples are necessary to initiate further node splitting. The `random_state` parameter is set to 42, ensuring reproducibility.
- The classifier built with TPOP for 100-node instances is implemented as an ExtraTreesClassifier that features bootstrapping. The entropy criterion is used to evaluate split quality across the trees. It also requires 80% of the features to be considered for each tree split and a minimum of 19 samples for each leaf node. Additionally, a node split requires at least 5 samples to proceed. The ensemble includes 100 trees, and the `random_state` parameter is fixed at 42.

The models with hyperparameters constructed in the section of RQAOA as a high-performing heuristic with the machine learning pipeline are highlighted in the following:

- The classifier configured for 20-node instances using the TPOP library employs a sequential machine-learning pipeline. It begins with a StackingEstimator that deploys an MLPClassifier, characterized by a learning rate of 1.0 and a low regularization factor. This is complemented by another StackingEstimator, which utilizes an ExtraTreesClassifier. This classifier uses the entropy criterion method, avoids bootstrapping, and considers 65% of the features during each split, all while adhering to predefined parameters for sample splits and minimum leaf size. The data is then normalized using a StandardScaler to ensure the features are optimally scaled. Finally, the process culminates with a GaussianNB classifier.
- The classifier configured using TPOP for 100-node instances also employs a sequential machine-learning pipeline. Initially, a StackingEstimator incorporating a GaussianNB classifier makes preliminary predictions that feed into later stages. Following that, a SelectFwe feature selector uses the `f_classif` with an alpha of 0.012 to selectively maintain features. Subsequently, another StackingEstimator featuring a Decision Tree Classifier is used, which is tailored with the Gini index for node splitting, a cap of 7 on tree depth, a minimum of 9 samples per leaf, and at least 12 samples required for further splitting. A RobustScaler is then employed to adjust feature scales. The process concludes with a GaussianNB classifier.